A measurement of the Michel parameters and the chirality parameter in $e^+e^- \to \tau^+\tau^-$ with the L3 Detector at LEP

The L3 Collaboration

Abstract

Using data collected with the L3 detector at LEP in 1991, 1992 and 1993, 34,000 events $e^+e^- \to \tau^+\tau^-$ have been selected. From the leptonic and hadronic τ decays, the Michel parameters (ρ, η, ξ and δ), the chirality parameter (ξ_h) and the τ polarization ($\mathcal{P}_\tau$) have been measured. We exploit for this analysis the energy spectra of leptons and hadrons from $\tau^- \to l^-\bar{\nu}_l\nu_\tau$ and $\tau^- \to \pi^-\nu_\tau$ decays, the energy and decay angular distributions in $\tau^- \to \rho^-\nu_\tau$ decays and the correlations in the energy spectra and angular distributions of the decay products.

Assuming electron-muon universality in the τ decay, the preliminary results for the Michel parameters are $\rho = 0.810 \pm 0.049$, $\eta = 0.10 \pm 0.23$, ξ=0.95$\pm$0.25 and $\xi\delta$=0.73$\pm$0.19, and the chirality parameter is ξ_h=-1.02 ± 0.08, in agreement with the V-A hypothesis for the weak charged current.

Submitted to the International Conference on High Energy Physics,
Brussels, 27th July through 2nd August 1995

1 Introduction

The subject of this paper is an investigation of the Lorentz structure of the charged current in the leptonic τ decays $\tau^- \to l^- \bar{\nu}_l \nu_\tau$ $(l = e, \mu)$ [1] and a measurement of the chirality parameter $\xi_h$in the hadronic τ decays $\tau^- \to h^- \nu_\tau$ $(h = \pi, \rho)$. This chirality parameter is interpreted as twice the average τ neutrino helicity. Because of the undetectable neutrinos and the unmeasured polarization of the outgoing lepton, only four Michel parameters [1] can be experimentally determined. Of these four parameters, ρ and η describe the isotropic part of lepton energy spectrum and ξ and δ describe the angular distribution with respect to the τ spin direction. Parity violation in τ decays was first observed by the ARGUS Collaboration at the DORIS II e^+e^- storage ring by a measurement of $\xi_h$in $\tau^- \to a_1^- \nu_\tau$ decays[2]. The lepton spectrum shape parameters ρ was measured by several experiments [3], [4] from e and μ energy spectra in τ decays. By using correlations between e and μ momenta in $e^+e^- \to \tau^+\tau^- \to (e^\pm \nu\bar{\nu})(\mu^\mp \nu\bar{\nu})$ ARGUS measured $|\xi|$ [4]. First measurements of η, ξ and δ were performed in $e^+e^- \to \tau^+\tau^- \to (l^\pm \nu\bar{\nu})(a_1^\mp \nu)$ [5] [6].

The parameters ξ and δ are easily accessible when the τ's are polarized. The LEP collider at CERN provides a clean source of polarized τ's produced in Z^0 decays. The average τ polarization was measured by the LEP collaborations to be $\mathcal{P}_\tau \simeq -0.14$. This confirms that parity is violated in τ production and decay [7, 8, 9, 10]. From LEP and SLD results on $\mathcal{P}_\tau$ and A_{LR} [11], respectively, the sign of $\mathcal{P}_\tau$ is defined to be negative, thus fixing the sign of ξ_h. This is in agreement with the first measurement of $\xi_h$by ARGUS [2]. At high energies the helicities of the τ's in $e^+e^- \to \tau^+\tau^-$ are almost completely anti-correlated. Energy spectra of leptons and hadrons from exclusive τ decays and the correlations between them allow the determination of four Michel parameters and the chirality parameter simultaneously. Results from the ALEPH experiment at LEP about the Lorentz structure in τ decays have been published recently [12].

2 Method of the Measurement

At the Born level, the most general matrix element for leptonic τ decays can be written as [13]

[1] If not stated otherwise, charge conjugate states are also implied throughout this paper.

$$\mathcal{M} = \frac{4G_F}{\sqrt{2}} \sum_{\substack{\gamma=S,V,T \\ \epsilon,\mu=R,L}} g^{\gamma}_{\epsilon\mu} < \bar{l}_{\epsilon}|\Gamma^{\gamma}|(\nu_l)_n >< (\overline{\nu}_{\tau})_m|\Gamma_{\gamma}|\tau_{\mu} > \tag{1}$$

Here γ labels the scalar, vector and tensor interactions and ϵ, μ the chiral projections of the charged leptons. The helicities of the neutrinos are fixed when γ is given. The 10 complex coupling constants $g^{\gamma}_{\epsilon\mu}$ can be expressed in terms of Michel parameters. Four of them, ρ, η, ξ and δ, appear in the charged lepton decay spectrum of the τ in the following form:

$$\begin{aligned} \frac{1}{\Gamma}\frac{d\Gamma(\tau^- \to l^-\bar{\nu}_l\nu_{\tau})}{dx} &= h_0(x) + \eta h_{\eta}(x) + \rho h_{\rho}(x) \\ &\quad -\mathcal{P}_{\tau}\ [\xi h_{\xi}(x) + \xi\delta h_{\xi\delta}(x)] \end{aligned} \tag{2}$$

where $x = \frac{E_l}{E_{\tau}}$ is the normalized lepton energy. In a similar way the hadronic τ decays can be described with a matrix element ansatz leading to the relation:

$$\frac{1}{\Gamma}\frac{d\Gamma(\tau^- \to h^-\nu_{\tau})}{dx} = h_0(x) + \mathcal{P}_{\tau}\ \xi_h h_1(x) \tag{3}$$

where $\xi_h$is the chirality parameter for a particular decay. For the $\tau^- \to \pi^-\nu_{\tau}$ decay, $h_0(x) = 1$ and $h_1(x) = (2x-1)$, where $x = \frac{E_{\pi}}{E_{\tau}}$. In the case of the $\tau^- \to \rho^-\nu_{\tau}$ decay a variable ω is introduced as a polarization analyser and h_0 and h_1 are functions of ω [14].

Assuming only vector and axial vector couplings in the decay $Z \to \tau^+\tau^-$, the helicities of the τ's are nearly 100% anti-correlated. When we consider the decays of both τ's in $e^+e^- \to \tau^+\tau^- \to A^+B^-\nu' s$, where A and B is an identified charged lepton or hadron, the joint decay distribution can be written as:

$$\begin{aligned} \frac{1}{\Gamma}\frac{d^2\Gamma}{dx_A dx_B} &= \mathrm{H}_0^{(A)}(x_A)\mathrm{H}_0^{(B)}(x_B) + \mathrm{H}_1^{(A)}(x_A)\mathrm{H}_1^{(B)}(x_B) \\ &\quad + P_{\tau}\left[\mathrm{H}_1^{(A)}(x_A)\mathrm{H}_0^{(B)}(x_B) + \mathrm{H}_0^{(A)}(x_A)\mathrm{H}_1^{(B)}(x_B)\right] \end{aligned} \tag{4}$$

For leptons, the H functions can be decomposed as follows:

$$\mathrm{H}_0^{(l)}(x) = \mathrm{h}_0^{(l)}(x) + \rho_l\,\mathrm{h}_{\rho}^{(l)}(x) + \eta_l\,\mathrm{h}_{\eta}^{(l)}(x) \tag{5}$$

$$\mathrm{H}_1^{(l)}(x) = \xi_l\,\mathrm{h}_{\xi}^{(l)}(x) + \xi_l\delta_l\,\mathrm{h}_{\xi\delta}^{(l)}(x) \tag{6}$$

with $\int\mathrm{h}_0(x)\,dx = 1$, $\int\mathrm{h}_{\eta}(x)\,dx = 4\frac{m_l}{m_{\tau}}$ and $\int\mathrm{h}_{\rho}(x)\,dx = \int\mathrm{h}_{\xi}(x)\,dx = \int\mathrm{h}_{\xi\delta}(x)\,dx = 0$.

In case of hadrons ($j = \pi, \rho$)

$$\mathrm{H}_0^{(j)}(x) = \mathrm{h}_0^{(j)}(x) \tag{7}$$

$$\mathrm{H}_1^{(j)}(x) = \xi_h \, \mathrm{h}_1^{(j)}(x) \tag{8}$$

with $\int \mathrm{h}_0(x)\, dx = 1$ and $\int \mathrm{h}_1(x)\, dx = 0$.

3 The L3 detector

Starting from the interaction point, the L3 detector is composed of the following subdetectors: a central tracking chamber consisting of a time expansion chamber (TEC) surrounded by two thin proportional chambers (Z-Chamber), a fine grained electromagnetic calorimeter (ECAL) composed of Bismuth Germanium Oxide (BGO) crystals, scintillation counters, a uranium and brass hadron calorimeter with proportional wire chambers readout (HCAL) and a precise muon spectrometer (MUCH) consisting of multiwire drift chambers.

These subdetectors are installed in a 12 m diameter solenoidal magnet which provides a uniform field of 0.5 T along the beam direction. A detailed description of the L3 detector and its perfomance is given elsewhere [15]. In the following analysis only the barrel part of the detector with $|\cos\theta| < 0.7$ is used.

4 Data analysis

A data sample corresponding a total integrated luminosity of 74.0 pb^{-1} collected by the L3 experiment during 1991, 1992 and 1993 data taking periods is used in this analysis. The selection of τ pairs produced in Z^0 decays, particle identification, τ decay mode classification and background rejection are similar to the ones descibed in [16]. First, leptonic Z^0 decays are selected by accepting only low multiplicity events with 'back to back' topology. Cosmic muons are rejected by the requirement that tracks originate from the nominal interaction point. Then each event is divided in two hemispheres by a plane perpendicular to the thrust axis. In each hemisphere, particles are identified independently.

4.1 Lepton identification

An electron signature is a track in the central tracker consistent in position and energy with an electromagnetic cluster in the BGO. The probability of matching between the measured track momentum and the BGO energy is calculated by maximizing the likelihood of these two measurements to originate from a single electron. The transverse shower shape of the ECAL cluster must be consistent with an electromagnetic shower.

Muons are identified as a track in the muon spectrometer matching to a track in the central tracker with a minimum ionizing particle response in ECAL and HCAL. Only muons with track segments in all three chamber planes of the muon spectrometer are accepted.

4.2 Hadron identification

The selection of $\tau^- \to \pi^- \nu_\tau$ and $\tau^- \to \rho^- \nu_\tau$ uses the central tracker and the calorimeters. First the impact point of the charged track at the ECAL is determined. Then an algorithm [16] for resolving overlapping neutral clusters in the vicinity of hadronic showers in the ECAL is applied in order to determine the numbers of neutral clusters, their energies and angles. Two distinct neutral clusters form a π^0 candidate if their invariant mass is within 40 MeV of the π^0 mass. A single neutral cluster forms a π^0 candidate if its energy exceeds 1 GeV and its transverse energy profile is consistent with an electromagnetic profile or the estimate of its invariant mass from a fit of its transverse profile with a two photon hypothesis is within 50 MeV of the π^0 mass. The sum of energies of reconstructed neutral clusters is subtracted from the energy of the ECAL and the remaining energy together with the deposition in the HCAL is assigned to the charged hadron. This measurement is then combined with the measurement of the momentum in the tracking chamber by maximizing the likelihood for these two measurements to originate from a single hadron.

The $\tau^- \to \pi^- \nu_\tau$ selection admits no π^0 candidates and no neutral clusters with energy greater than 0.5 GeV. To select $\tau^- \to \rho^- \nu_\tau$ decays, exactly one π^0 candidate is required in the hemisphere. The invariant mass of the $\pi^- \pi^0$ system must be in the range 0.45 to 1.20 GeV.

Selection efficiencies are calculated using fully simulated $e^+e^- \to \tau^+\tau^-$ events. These events are also used in order to estimate the background from other τ decay modes in the selected final states. Few events survive the criteria for two particle identifications simultaneously. 0.55% of electrons are also identified as pions, 0.07% of electrons as rhos, 0.25% of muons as pions, 0.84% of muons as rhos and 0.01% pions as rhos. These events are assigned to the electron, muon and π sample, respectively. The particle identification efficiencies and the remaining backgrounds from other τ decays are shown in table 1.

Events with at least one identified leptonic or hadronic τ decay are retained and classified into the following exclusive groups: $e\mu$, $e\pi$, $e\rho$, ee, $\mu\mu$, $\mu\pi$, $\mu\rho$, $\pi\pi$, $\pi\rho$, $\rho\rho$, eX, μX, πX and ρX, where X stands for an unidentified one-prong τ decay.

The background from other than $e^+e^- \to \tau^+\tau^-$ final states is estimated in each channel from data using the opposite hemisphere particle spectra and global event charactersitics. The number of selected events in each category, the selection efficiencies and background estimates are summarized in table 2.

5 Measurement of Michel parameters, τ polarization and the chirality parameter

We extract values of ρ,η, ξ and δ, $\mathcal{P}_\tau$ and $\xi_h$from a binned maximum likelihood fit to the one-dimensional energy spectra of eX and μX and πX, the spectrum of the ω variable of the ρ and to the joint decay distributions of all combinations of e, μ, π and ρ in the final state.

The likelihood function is defined as:

$$\mathcal{L} = \prod_{ij} \frac{w_{ij}^{n_{ij}} e^{-w_{ij}}}{n_{ij}!}$$

where i runs over the single particle spectra and j runs over the bins of the two dimensional distributions included in the fit. The n_{ij} is the number of data events observed in bin j of the i-th decay mode and $w_{ij}(\rho,\eta,\xi,\xi\delta,\mathcal{P}_\tau\ ,\xi_h)$ is the expected number of events. The w_{ij} are normalized;

	selection efficiency (%)	background from other τ decays (%)
$\tau^- \to e^-\bar{\nu}_e\nu_\tau$	56	1.9
$\tau^- \to \mu^-\bar{\nu}_\mu\nu_\tau$	58	1.0
$\tau^- \to \pi^-\nu_\tau$	42	10.
$\tau^- \to \rho^-\nu_\tau$	41	13.

Table 1: Particle identification efficiencies and background fractions from other τ decays in exclusive final states. Included is the inefficiency due to selecting events in the range $|\cos\theta| < 0.7$ only.

$Z^0 \to \tau^+\tau^-$	events	selection efficiency (%)	background from other τ decays (%)	background from non τ decays (%)
ee	1157	41.3	3.4	2.0
eμ	1453	43.9	2.9	0.5
eπ	1205	35.0	10.7	0.2
eρ	2358	32.8	14.4	0.2
e X	6275	51.0	1.9	5.0
$\mu\mu$	590	36.9	1.1	3.0
$\mu\pi$	889	35.3	10.5	1.0
$\mu\rho$	1818	32.2	13.9	1.0
μ X	4097	53.3	1.0	3.5
$\pi\pi$	440	30.6	17.2	0.5
$\pi\rho$	1526	27.9	21.0	0.2
π X	3622	40.5	10.5	0.2
$\rho\rho$	1615	26.2	24.0	0.1
ρ X	6764	41.0	13.2	0.1
total	33809			

Table 2: The number of events, the selection efficiencies and background contents in selected exclusive channels

$$\sum_{ij} w_{ij} = N_i$$

where N_i is total number of data events in i-th distribution.

The expected number of events, w_{ij}, is obtained in the following procedure. The functions $h_0^{(l)}$, $h_\rho^{(l)}$, $h_\eta^{(l)}$, $h_\xi^{(l)}$, $h_{\xi\delta}^{(l)}$, $h_0^{(j)}$ and $h_1^{(j)}$ of eqns. (5)-(8) are obtained from the KORALZ Monte Carlo Generator [17] with a modified version of the τ decay Monte Carlo package TAUOLA [18]. For each leptonic decay channel, 5 samples of events corresponding to the settings of the Michel parameters given in table 3 are generated.

From differences in the distributions S1 through S5, the $h_i^{(l)}(x)$ are constructed. Initial and final state QED radiative corrections, radiation in the decay $\tau^- \to l^-\bar{\nu}_l\nu_\tau$, and effects of the lepton masses m_e and m_μ are included.

As an illustration, the shape of the functions $h_0^{(\mu)}(x), h_\rho^{(\mu)}(x), h_\eta^{(\mu)}(x), h_\xi^{(\mu)}(x)$ and $h_{\xi\delta}^{(\mu)}(x)$ are shown in fig. 1 for the muon channel. The solid lines are the result of

	ρ	η	ξ	$\xi\delta$
S1	0	0	0	0
S2	0	1	0	0
S3	0.75	0	0	0
S4	0	0	1	0
S5	0.5	0	0	0.5

Table 3: Settings of the Michel parameters in TAUOLA for auxiliary distributions used to construct the $h_i^{(l)}$ functions

the Born approximation [19]. The shapes extracted from the MC are similar to the analytic Born-level results. Radiative corrections do not distort the spectra very much. The functions for the electron decay are very similar, but the function $h_\eta(x)$ contains a suppresion factor $\frac{m_l}{m_\tau}$, so that for $\tau^- \to e^-\bar{\nu}_e\nu_\tau$ the sensitivity to η is strongly reduced. For the $\tau^- \to h^-\nu_\tau$ decays, $h_0^{(j)}(x)$ and $h_1^{(j)}(x)$, obtained in a similar way, are shown in fig. 2 for the π and in fig. 3 for the ρ.

The theoretical decay spectra are then folded with the experimental resolutions and acceptances. First, eqns. (5)-(8) are used to construct a probability distribution T, where

$$T(x,\rho,\eta,\xi,\xi\delta,\mathcal{P}_\tau\ ,\xi_h) = H_0(x) + \mathcal{P}_\tau\ H_1(x) \tag{9}$$

for e X, μX, πX and ρX final states and

$$\begin{aligned} T(x_A,x_B,\rho,\eta,\xi,\xi\delta,\mathcal{P}_\tau\ ,\xi_h) \quad = \quad & \mathrm{H}_0^{(A)}(x_A)\mathrm{H}_0^{(B)}(x_B) + \mathrm{H}_1^{(A)}(x_A)\mathrm{H}_1^{(B)}(x_B) \\ & + \mathcal{P}_\tau\ \left[\mathrm{H}_1^{(A)}(x_A)\mathrm{H}_0^{(B)}(x_B) + \mathrm{H}_0^{(A)}(x_A)\mathrm{H}_1^{(B)}(x_B)\right] \end{aligned} \tag{10}$$

for the double sided final states.

T is then subjected to detector resolution and acceptance corrections;

$$S = \epsilon(x^{rec}) \otimes R(x^{rec},x^{gen}) \otimes T \tag{11}$$

where $\epsilon(x^{rec})$ and $R(x^{rec},x^{gen})$ are the acceptance and resolution functions of the detector. The w_{ij} are obtained from

$$w_{ij}(\mathcal{P}_\tau\ ,\rho,\eta,\xi,\delta,\xi_h) = \int_{bin}\{S(x,\mathcal{P}_\tau\ ,\rho,\eta,\xi,\delta\xi_h)\}dx + b_{ij} \tag{12}$$

where b_{ij} represents the background in the corresponding bin.

In the hadronic decay modes, an alternate method has been used to obtain w_{ij} of eqn. (12) as a cross check of the method described above. In this approach, we obtain the distributions from fully simulated Monte Carlo events. The functions $h_0^{(j)}$ and $h_1^{(j)}$ are the properly weighted sum or difference of the contributions from positive and negative τ^- helicity states, respectively. QED radiative corrections, detector resolution, and selection efficiencies are taken into account.

6 Systematic errors

Systematic errors are estimated for the selection procedure, the background fractions, and the uncertainty in the calibration of the subdetectors as described in [9]. The non-τ background fraction normalization is assumed to be known within $\pm 10\%$. The accuracy of the BGO energy scale is estimated to be 1% at 1 GeV and 0.1% at 45 GeV. The momentum scale of the central tracker is known to within 1%, and for the muon chambers to within 0.2% at 45 GeV. At low momenta, the muon momentum uncertainty is dominated by energy losses in the calorimeters, which is known to an accuracy of 50 MeV.

7 Result and discussion

In a first fit we determine the chirality parameter $\xi_h$and the τ polarization $\mathcal{P}_\tau$ from the final states πX, ρX, $\pi\pi$, $\rho\rho$ and $\rho\pi$ using the full detector simulation. As an example of the joint decay distributions, we show in fig. 5 the pion energy spectrum for different slices of the ω variable and vice versa for the $(\tau^- \to \pi^- \nu_\tau)(\tau^- \to \rho^- \nu_\tau)$ final state. The spin correlations are clearly visible. The fit describes the data well, in the one dimensional distributions as well as in the correlated spectra. The values obtained for $\mathcal{P}_\tau$ and ξ_h, using fully simulated spectra, are $-0.170 \pm 0.017 \pm 0.014$ and $-0.92 \pm 0.05 \pm 0.06$ respectively. The χ^2 per degree of freedom is 1.01 and the correlation coefficient -0.467.

A common fit to all leptonic and hadronic decay channels results in a measurement of the Michel parameters ρ, η, ξ and $\xi\delta$, the chirality parameter in hadronic decays, $\xi_h$and the τ polarization $\mathcal{P}_\tau$. The results of the fit for one dimensional distributions of leptonic and hadronic spectra is shown fig. 4. The measurement and the prediction of the Standard Model are summarized in table 4. The χ^2 per degree of freedom resulting from the fit is 1.27, and correlation coefficients are listed in table 5.

	this measurement	SM prediction
ρ	0.810$\pm$ 0.042$\pm$ 0.025	0.75
η	0.10 $\pm$ 0.18 $\pm$ 0.15	0.0
ξ	0.95 $\pm$ 0.23 $\pm$ 0.10	1.0
$\xi\delta$	0.73 $\pm$ 0.16 $\pm$ 0.10	0.75
ξ_h	-1.02 $\pm$ 0.06 $\pm$ 0.06	-1.0
$\mathcal{P}_\tau$	-0.135$\pm$ 0.024$\pm$ 0.012	

Table 4: The results for the Michel parameters, the chirality parameter $\xi_h$and the τ polarization $\mathcal{P}_\tau$ and their prediction of the Standard Model. The first error is statistical and the second systematic.

corr.	ρ	η	ξ	$\xi\delta$	ξ_h
$\mathcal{P}_\tau$	0.539	0.059	0.274	-0.411	-0.454
ρ		0.455	-0.062	-0.366	-0.365
η			0.135	0.053	-0.030
ξ				-0.001	0.065
$\xi\delta$					0.433

Table 5: The correlation coefficients for the Michel parameters, the chirality parameter $\xi_h$and the τ polarization $\mathcal{P}_\tau$.

Both measurements are in agreement with the predictions of pure V-A couplings in leptonic and semi-leptonic τ decays.

8 Acknowledgements

We wish to express our gratitude to the CERN Accelerator Division for the excellent performance of the LEP machine. We acknowledge the efforts of all engineers and technicians who have participated in the construction and maintenance of this experiment.

References

[1] L.Michel,*Proc. Phys. Soc. A63* (1950) 514.

[2] ARGUS Collab., H.Albrecht et al., Phys.Lett. B250 (1990) 164; Z.Phys. C58 (1993) 61.

[3] W. Bacino et al., Phys. Rev. Lett. 42 (1979) 749.
S. Behrends et al., Phys. Rev. D32 (1985) 2468.
W. T. Ford et al., Phys. Rev. D36 (1987) 1971.
H. Janssen et al., Phys. Lett. B228 (1989) 273.

[4] ARGUS Collab., H.Albrecht et al., Phys.Lett. B316 (1993) 608;

[5] ARGUS Collab., H. Albrecht et al., Phys. Lett. B341 (1995) 441.

[6] ARGUS Collab., H.Albrecht et al., Phys. Lett. B349 (1995) 576.

[7] ALEPH Collab., D.Buskulic et al., Z.Phys. C59 (1993) 369;
CERN-PPE/95-023, subm. to Z. für Physik C.

[8] DELPHI Collab., P.Abreu et al., Z.Phys. C55 (1992) 555.
CERN-PPE/95-30, subm. to Z. für Physik C.

[9] L3 Collaboration, M.Acciarri *et al.*, *Phys. Lett.* **B341** (1994) 245.

[10] OPAL Collab., G.Alexander et al., Phys.Lett. B266 (1991) 201.

[11] SLD Collab., K.Abe et al., Phys. Rev. Lett. 70 (1993) 2515.

[12] ALEPH Collab., D. Busculic et al., Phys. Lett. B346 (1995) 379.

[13] F. Scheck, Phys. Rep. 44 (1978) 187; Leptons, Hadrons and Nulei, North Holland Physics Publishing, Amsterdam (1983)
W. Fetscher, Phys. Rev. D 42 (1990) 1544.
C.Nelson, Phys. Rev. D40 (1989) 123.

[14] M. Davier, L. Duflot, F. Le Diberder and A. Rougé, Phys.Lett. B 306 (1993) 411.

[15] L3 Collab., B.Adeva et al., Nucl. Inst. and Meth. A289 (1990) 35.

[16] L3 Collab., O.Adriani et al., Phys.Lett. B294 (1992) 466.

[17] S. Jadach, B. F. L. Ward, Z. Was, Comp. Phys. Comm. 66 (1991) 276.

[18] M.Schmidtler, *A Convenient Parametrization for the General Matrix Element of Leptonic Tau Decay*, University Karlsruhe preprint IEKP-KA/93-14 (July 1993) (unpublished)

[19] S. Jadach, Z. Was et al. in 'Z Physics at LEP1', CERN Report CERN-89-08, eds. G. Altarelli, R. Kleiss and C. Verzegnassi (CERN, Geneva, 1989) Vol. 1, p. 235.

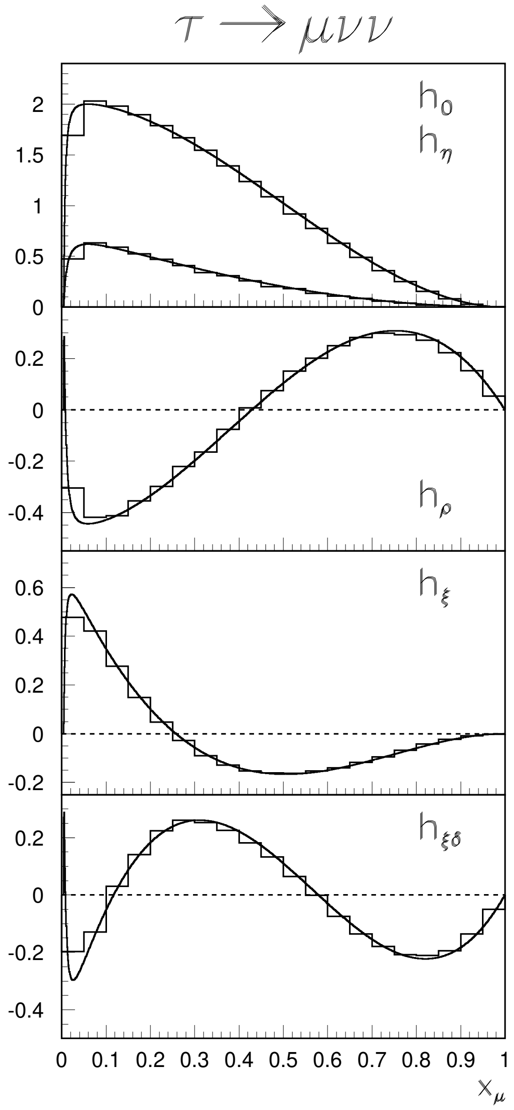

Figure 1: The functions $h_0^{(\mu)}(x), h_\rho^{(\mu)}(x), h_\eta^{(\mu)}(x), h_\xi^{(\mu)}(x)$ and $h_{\xi\delta}^{(\mu)}(x)$ for the $\tau^- \to \mu^- \bar{\nu}_\mu \nu_\tau$ decay. The solid lines are Born level calculations.

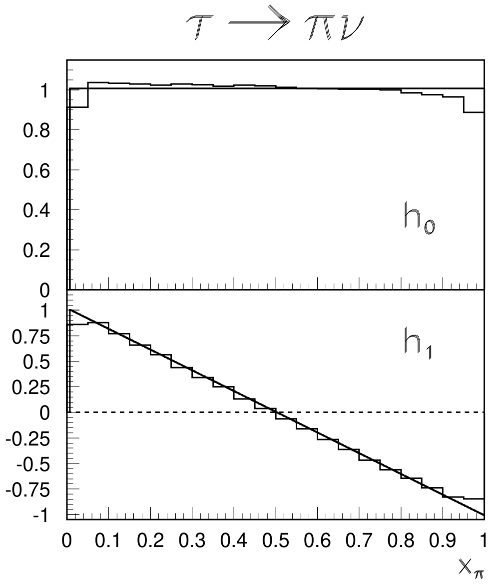

Figure 2: The functions $h_0^{(\pi)}(x)$ and $h_1^{(\pi)}(x)$ for the $\tau^- \to \pi^- \nu_\tau$ decay. The solid lines are Born level calculations.

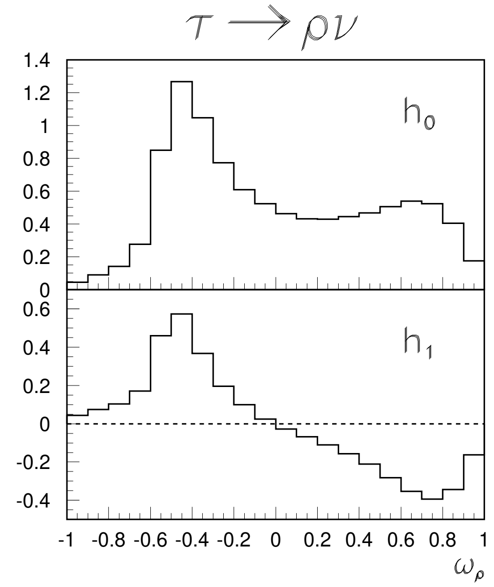

Figure 3: The functions $h_0^{(\rho)}(x)$ and $h_1^{(\rho)}(x)$ for the $\tau^- \to \rho^- \nu_\tau$ decay.

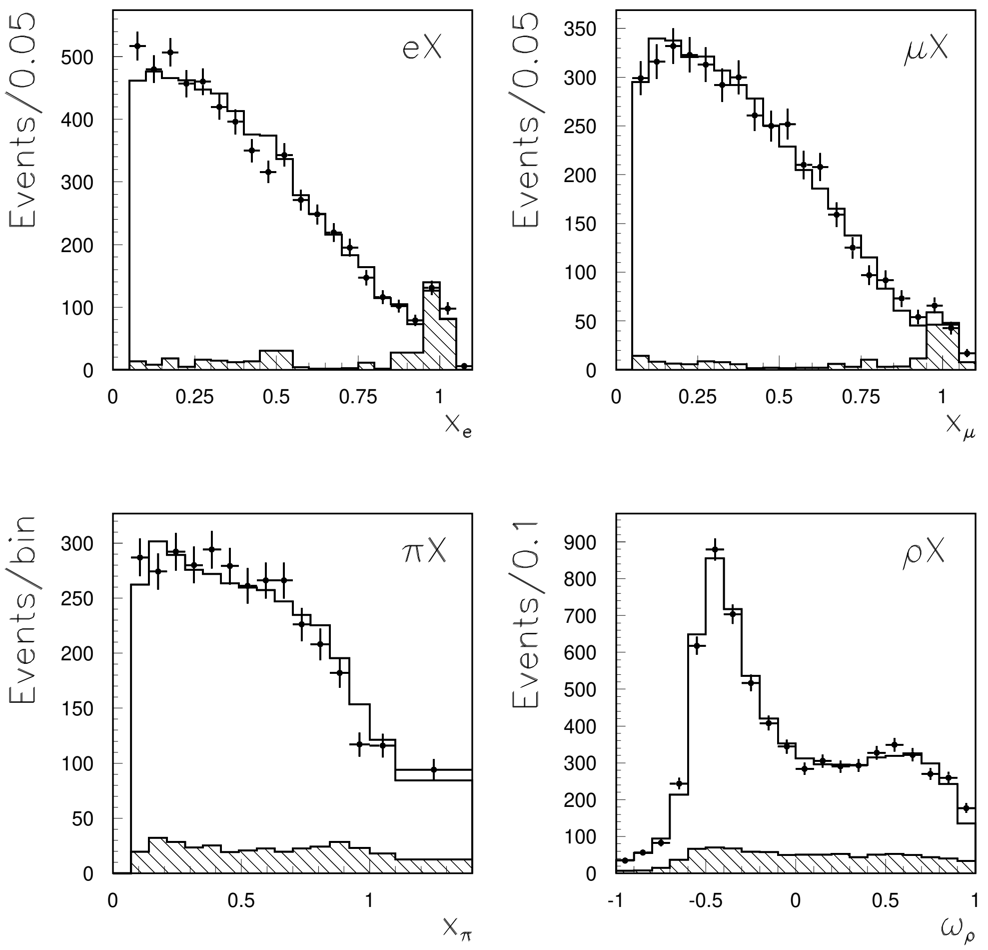

Figure 4: eX, μX, πX and ρX data (dots) with results of the fits (solid histogram) superimposed. τ and non-τ background are shown as hatched histograms respectively.

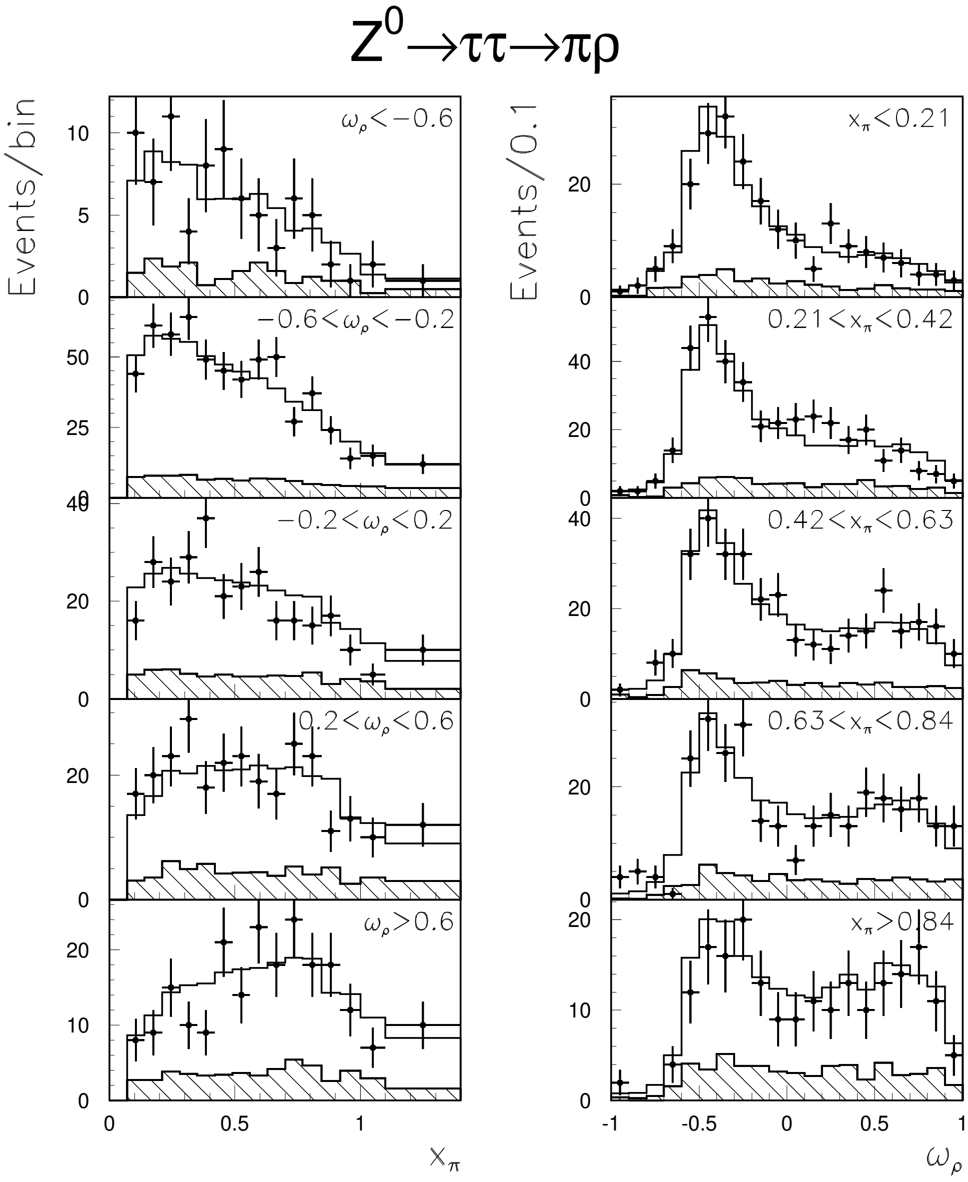

Figure 5: π and ρ spectra from $e^+e- \rightarrow \tau^+\tau^- \rightarrow \pi\rho\nu$'s (dots) for slices in the spin analyser ω (ρ) or the normalized momentum (π) on the opposite side, respectively, with result of the fit (solid histogram) superimposed. τ and non-τ background are shown as hatched histograms respectively.